Acta Biochim Biophys Sin 2024, 56(2): 280–290
https://doi.org/10.3724/abbs.2023275
Advance Access Publication Date: 25 January 2024
Original Article

Original Article

Human umbilical cord mesenchymal stem cells protect against ferroptosis in acute liver failure through the IGF1-hepcidin-FPN1 axis and inhibiting iron loading

Haiqin Cheng[1,2,3,4], Yaqian Shi[1,2,3], Xuewei Li[1,2,3], Ning Jin[1,2,3], Mengyao Zhang[1,2,3], Zhizhen Liu[1,2,3,*], Yuxiang Liang[1,3,5,*], and Jun Xie[1,2,3,*]

[1]Shanxi Key Laboratory of Birth Defect and Cell Regeneration, Shanxi Medical University, Taiyuan 030001, China, [2]Department of Biochemistry and Molecular Biology, Shanxi Medical University, Taiyuan 030001, China, [3]Key Laboratory of Coal Environmental Pathogenicity and Prevention, Shanxi Medical University, Ministry of Education, Taiyuan 030001, China, [4]Department of Medical, Fenyang Hospital of Shanxi Province, Lvliang 032200, China, and [5]Experimental Animal Center of Shanxi Medical University, Shanxi Key Laboratory of Human Disease and Animal Models, Taiyuan 030001, China

*Correspondence address. Tel: +86-351-3985008; E-mail: junxie@sxmu.edu.cn (J.X.) / E-mail: liangyuxiang@sxmu.edu.cn (Y.L.) / E-mail: zhizhenliu2013@163.com (Z.L.)

Received 22 July 2023 Accepted 28 September 2023

Abstract

Acute liver failure (ALF) is a significant global issue with elevated morbidity and mortality rates. There is an urgent and pressing need for secure and effective treatments. Ferroptosis, a novel iron-dependent regulation of cell death, plays a significant role in multiple pathological processes associated with liver diseases, including ALF. Several studies have demonstrated that mesenchymal stem cells (MSCs) have promising therapeutic potential in the treatment of ALF. This study aims to investigate the positive effects of MSCs against ferroptosis in an ALF model and explore the underlying molecular mechanisms of their therapeutic function. Our results show that intravenously injected MSCs protect against ferroptosis in ALF mouse models. MSCs decrease iron deposition in the liver of ALF mice by downregulating hepcidin level and upregulating FPN1 level. MSCs labelled with Dil are mainly observed in the hepatic sinusoid and exhibit colocalization with the macrophage marker CD11b fluorescence. ELISA demonstrates a high level of IGF1 in the CCL_4 + MSC group. Suppressing the IGF1 effect by the PPP blocks the therapeutic effect of MSCs against ferroptosis in ALF mice. Furthermore, disruption of IGF1 function results in iron deposition in the liver tissue due to impaired inhibitory effects of MSCs on hepcidin level. Our findings suggest that MSCs alleviate ferroptosis induced by disorders of iron metabolism in ALF mice by elevating IGF1 level. Moreover, MSCs are identified as a promising cell source for ferroptosis treatment in ALF mice.

Key words mesenchymal stem cell, acute liver failure, ferroptosis, iron loading, insulin-like growth factor-1

Introduction

Acute liver failure (ALF) represents a potentially life-threatening condition characterized by sudden onset, rapid deterioration, numerous complications, and alarmingly high mortality rates [1]. ALF worldwide is estimated to affect approximately 1 to 6 individuals per million annually [2]. While liver transplantation remains the most effective treatment for ALF, its accessibility is hindered by the severity and rapid progression of patients' illnesses, coupled with the scarcity of available donor organs. Furthermore, even after successful liver transplantation, the disease mortality rate can still reach up to 30% [3]. Regrettably, recent years have witnessed minimal progress in improving the survival rates of ALF patients [4,5]. Therefore, there is an imperative need to explore high-efficiency nonsurgical treatment to improve the overall prognosis of patients.

Ferroptosis is a recently discovered iron-dependent nonapoptotic programmed cell death mechanism [6]. Recent studies have shown that the characteristics of ferroptosis are found in different stages of

liver diseases, encompassing iron metabolism disorder, imbalance of the antioxidant system and lipid peroxide accumulation [7]. Brent R. Stockwell identified metabolism, ROS, and iron biology as pivotal regulators of ferroptosis [8]. Moreover, a plethora of studies have also demonstrated that intracellular iron-loading status is necessary for intracellular ferroptosis [9,10]. Furthermore, it has been discovered that intracellular iron overload, which is mediated by hepcidin and ferroportin (FPN1), is the key link to the occurrence of ferroptosis [8,11]. Hepcidin, a circulating hormone primarily produced by the liver, strictly regulates systemic iron metabolism in mammals [12]. FPN1 is currently recognized as the exclusive iron export channel from cells into the plasma. The structure of hepcidin-bound FPN1 unveils iron homeostatic mechanisms, hepcidin binds to FPN1 in an outwards-open conformation to negatively regulate FPN1, and it completely occludes the iron efflux pathway by inhibiting iron transport [13–15]. A deficient hepcidin response to iron loading may result in systemic iron overload [16], whereas transgenic mice overexpressing hepcidin experience severe iron deficiency anemia [17]. In humans, juvenile hemochromatosis, caused by loss-of-function mutations in hepcidin, results in severe iron deposition and multiple organ damage, including afflictions of the liver, heart, and endocrine tissues [18]. In mice with subarachnoid hemorrhage treated with heparin (an inhibitor of hepcidin), downregulating the expression of hepcidin and increasing FPN1 level could exert protective effects against ferroptosis following subarachnoid hemorrhage [15]. Furthermore, several studies have indicated a negative association between FPN1 and ferroptosis. For example, *FPN1* knockout in the brain microvasculature decreased brain iron level and inhibited ferroptosis in ischemic stroke mice [19]. Moreover, activation of the NRF2/FPN1 pathway mitigated myocardial ischemia-reperfusion injury in diabetic rats by regulating iron homeostasis and ferroptosis [20].

Stem-cell therapy has great promise and has been revealed as a therapeutic option for ALF [21,22]. After investigating different types of stem cells, researchers have determined that human umbilical cord-derived mesenchymal stem cells (H-uc MSCs) are an appropriate treatment option, as these cells can be easily obtained and are characterized by their high quality, purity, and abundance. Simultaneously, MSCs have emerged as highly viable alternatives in clinical practice. Meanwhile, stem cell-derived hepatocyte therapy could also effectively treat ALF [23,24]. Currently, 163 ongoing clinical trials use MSCs to treat different liver diseases, including ALF (https://clinicaltrials.gov/; Accessed 13 December 2021). In patients with ALF, the therapeutic effect of MSCs is satisfactory in the short term. Furthermore, it has been reported that MSCs play a protective role against ferroptosis by maintaining SLC7A11 function [25]. Furthermore, bone marrow-derived mesenchymal stem cells have been shown to alleviate ischemia-reperfusion injury following steatotic liver transplantation by inhibiting ferroptosis [26]. Currently, the primary mechanism by which MSCs protect against ferroptosis is through inhibiting lipid peroxidation rather than promoting intracellular iron export [26,27]. However, the focus of our study was mainly on MSCs that could inhibit ferroptosis by reducing intracellular iron level.

Several reports have underscored that the *in vivo* biological function of MSCs is closely associated with specific growth factors, such as insulin-like growth factor-1 (IGF1). In murine models of colitis, MSCs have been demonstrated to enhance colon epithelial integrity and regeneration through the elevation of hepatic secretion of IGF1 [28]. Likewise, H-uc MSCs exhibit the capacity to attenuate severe burn-induced multiple organ injury by increasing protective cytokine IGF1 level [29]. IGF1 also plays a crucial role in the pathological state of the liver. For example, in a liver injury model, treatment with a low dose of IGF1 has been demonstrated to repair the development of liver injury and reduce the severity of liver fibrosis [30,31]. Furthermore, IGF1 treatment could improve the biochemistry, histology, and genetic expression of proregenerative and cytoprotective factors in healthy and IGF1-deficient mice with acute liver damage [32]. However, there is limited experimental evidence to support the role of IGF1 in mediating the molecular mechanism of MSC therapy for ALF by protecting against ferroptosis.

This study aimed to delineate the effects of H-uc MSCs on ferroptosis in CCL_4-induced hepatotoxicity and elucidate the intricate mechanism involving the IGF1-hepcidin-FPN1 axis. Our study provides a valuable resource for deciphering the molecular mechanism that underlies the therapeutic effect of H-uc MSCs on ALF.

Materials and Methods

Extraction and identification of H-uc MSCs

Human umbilical cords were obtained through full-term caesarian section deliveries with the informed consent of the parents. MSCs from the umbilical cord were isolated and cultured using the method previously described by Fu *et al.* [33]. During MSC quality control, cultured cells at the fourth passage (P4) were assessed using osteogenic differentiation medium (A1007201; Gibco, New York, USA) and adipogenic differentiation medium (A1007001; Gibco) for differentiation capacity. The phenotype of MSCs was identified by flow cytometry on a FACS Celesta flow cytometer (BD, Franklin Lakes, USA). Oil red staining and alizarin red S staining were used to detect osteoblasts and adipocytes. The following antibodies obtained from BD were employed for flow cytometric analysis: CD90 (519007657), CD44 (519007656), CD73 (519007649), CD105 (519007648), and H-uc MSC Negative Cocktail (519007661). H-uc MSCs were labelled with a Dil fluorescent probe (C1036; Beyotime, Shanghai, China) following the protocols provided by the manufacturer, and the labelling efficiency was detected by flow cytometry.

Animal models and experimental design

Eight-week-old C57BL/6J male mice were purchased from Vital River Laboratory Animal Technology (Beijing, China) and randomly divided into three groups ($n = 10$ mice per group). These groups were designated as the negative control group (NC), ALF group (CCL_4 + PBS) and MSC treatment group (CCL_4 + MSC). In the NC group, mice were given 100 μL PBS through the tail vein. In the ALF group, mice were administered with 2.5 mL/kg CCL_4 via intraperitoneal (i.p.) injection, and then 100 μL PBS was injected via the tail vein after 3 h. In the MSC treatment group, mice were administered with 2.5 mL/kg CCL_4 via i.p. injection and 5×10^5 MSCs in 100 μL PBS via the tail vein after 3 h. Mice were sacrificed on day 3, and liver and serum samples were collected for further analysis.

For the IGF1 receptor inhibitor experiment, the IGF1 receptor inhibitor picropodophyllin (PPP; MedChemExpress, Monmouth Junction, USA) was utilized. The mice were randomly divided into four groups ($n = 10$ mice per group): the negative control group (NC), the ALF group (CCL_4 + PBS + vehicle), the MSC treatment

group (CCL_4 + MSC + vehicle), and the PPP group (CCL_4 + MSC + PPP). Mice in each experimental group received 1.25 mL/kg CCL_4 through i.p. injection. Mice in the PPP group (CCL_4 + MSC + PPP) were treated daily with30 mg/kg PPP and a single MSC injection of 5×10^5 cells via intraperitoneal administration. Mice in the ALF group (CCL_4 + PBS + vehicle) and the MSC group (CCL_4 + MSC + vehicle) were treated daily with inhibitor vehicles via intraperitoneal administration. Mice were sacrificed on day 3, and liver and serum samples were collected and stored at −80°C.

Measurement of serum malonaldehyde (MDA) and glutathione (GSH)

Serum was isolated from whole blood samples by centrifugation at 1900 *g* for 15 min. Serum MDA and GSH levels were examined using the MDA assay kit (TBA method) and the Reduced GSH assay kit (Nangjing Jiancheng Bioengineering Institute, Nangjing, China). The optical density values were measured with a SpectraMax190 microplate reader (Molecular Devices, Sunnyvale, USA).

Measurement of tissue iron

The liver proteins were extracted by the tissue homogenate method and detected using the BCA protein assay kit (PC0020; Solarbio, Beijing, China). Iron levels in the liver were measured using a tissue iron assay kit (Nanjing Jiancheng Bioengineering Institute). The optical density values were measured with a microplate reader.

ELISA for serum IGF1

Serum IGF1 concentrations were measured using the Mouse IGF1 ELISA kit (JL12620; Jianglaibio, Shanghai, China) following the manufacturer's protocols. The optical density values were measured with a microplate reader.

Hematoxylin-eosin (HE) staining

The left lobes of the liver were collected and fixed with 4% paraformaldehyde and then embedded in paraffin. Each tissue sample was sectioned into 4-μm-thick slices. The HE staining procedure was performed following the instructions of the Hematoxylin-Eosin Stain kit (G1120; Solarbio). Finally, the slides were subjected to observation with a PA53 biological microscope (Motic, Fuzhou, China).

Immunohistochemistry (IHC)

The slices on slides were subjected to dewaxing and rehydration. Subsequently, permeabilization was performed using 1% Triton X-100 (#T8200; Solarbio) and blocking was performed with 10% horse serum. Next, the sections were incubated overnight at 4°C with the following primary antibodies: Ptgs2 (1:200, ab283574; Abcam, Cambridge, UK), Gpx4 (1:200, ab125066; Abcam), hepcidin (1:200, AF7003; Affinity, Liyang, China), IGF-1R (1:200, AF6125; Affinity), P-IGF-1R (1:200, AF3123; Affinity), P-AKT (1:200, AF0016; Affinity), ferritin (1:100, ab287968; Abcam) and TfR1 (1:2000, ab269513; Abcam). Then, the HRP-conjugated secondary antibody (PV-6000; ZSGB-BIO, Beijing, China) was used for incubation at 37°C for 20 min. Reaction products were visualized by using 3,3′-diaminobenzidine (DAB). The images were captured with the PA53 biological microscope.

Prussian blue iron staining (Perl's staining)

The slices were subjected to dewaxing and rehydration. The Prussian blue iron staining procedure was performed following the instructions of the Prussian Blue Iron Stain kit (G1428; Solarbio). The results were measured using the PA53 biological microscope.

Immunofluorescence staining

The sections were subjected to dewaxing and rehydration and then permeabilized with 0.1% Triton X-100 for 10 min. Then, the sections were blocked for 1 h with 10% horse serum. The sections were incubated overnight with a FITC-conjugated anti-mouse/human CD11b primary antibody (1:100, 101205; Biolegend, San Diego, USA) at 4°C. Then the nuclei were stained with DAPI which contained an anti-fluorescence quenching sealant (BL739A; Biosharp, Hefei, China). Finally, the slides were examined with a FV1000 confocal laser scanning biological microscope (Olympus, Tokyo, Japan).

Western blot analysis

Liver proteins were isolated and collected using RIPA buffer (R0010, Solarbio) supplemented with 1 × protease inhibitor mixture (P6730; Solarbio). The total protein was quantified using a BCA Protein Assay kit. The proteins were separated by 10% SDS-PAGE and subsequently transferred onto PVDF membranes. The target protein was probed using the primary antibodies against hepcidin (1:500, AF7003; Affinity), BMP6 (1:500, AF5196; Affinity) and FPN1 (1:200, DF13561; Affinity). Subsequently, the membrane was incubated with the corresponding HRP-conjugated secondary antibody (1:10,000 in TBS-T buffer) for 2 h at room temperature. The protein bands were visualized using an Enhanced chemiluminescence (ECL) kit (Boster, Wuhan, China), and quantified with the ChemiDoc MP Imaging System (Bio-Rad, Hercules, USA). GAPDH was used as the internal control.

Statistical analysis

Data are presented as the mean ± SEM. The intergroup comparison was assessed by the *t* test in GraphPad Prism 8.0.1 (GraphPad Software, San Diego, USA). $P < 0.05$ was considered statistically significant.

Results

Characterization of H-uc MSCs

Under an optical microscope, the P4 H-uc MSCs were found to have adherent growth ability and a spindle-shaped appearance (Figure 1A). To identify the pluripotency of H-uc MSCs, we effectively induced their differentiation into both adipocytes and osteoblasts using specific differentiation media. Alizarin red S staining verified the deposition of red calcium salt and the formation of mineralized nodules (Figure 1B). The formation of lipid droplets was verified by Oil red O staining (Figure 1B). Subsequently, flow cytometry was employed to identify the phenotype markers of H-uc MSCs. As shown in Figure 1C, the percentages of CD105, CD90 and CD73-positive cells were 100%, 99.5%, and 99.9%, respectively, and the percentages of CD34, CD11b, CD19, CD45 and HLA-DR-negative cells were less than one percent. H-uc MSCs could be effectively labelled by Dil, and the labelling efficiency was approximately 99% (Figure 1D).

Ferroptosis occurred in CCL_4-induced ALF mice

As shown in Figure 2A, compared with the NC groups, typical liver

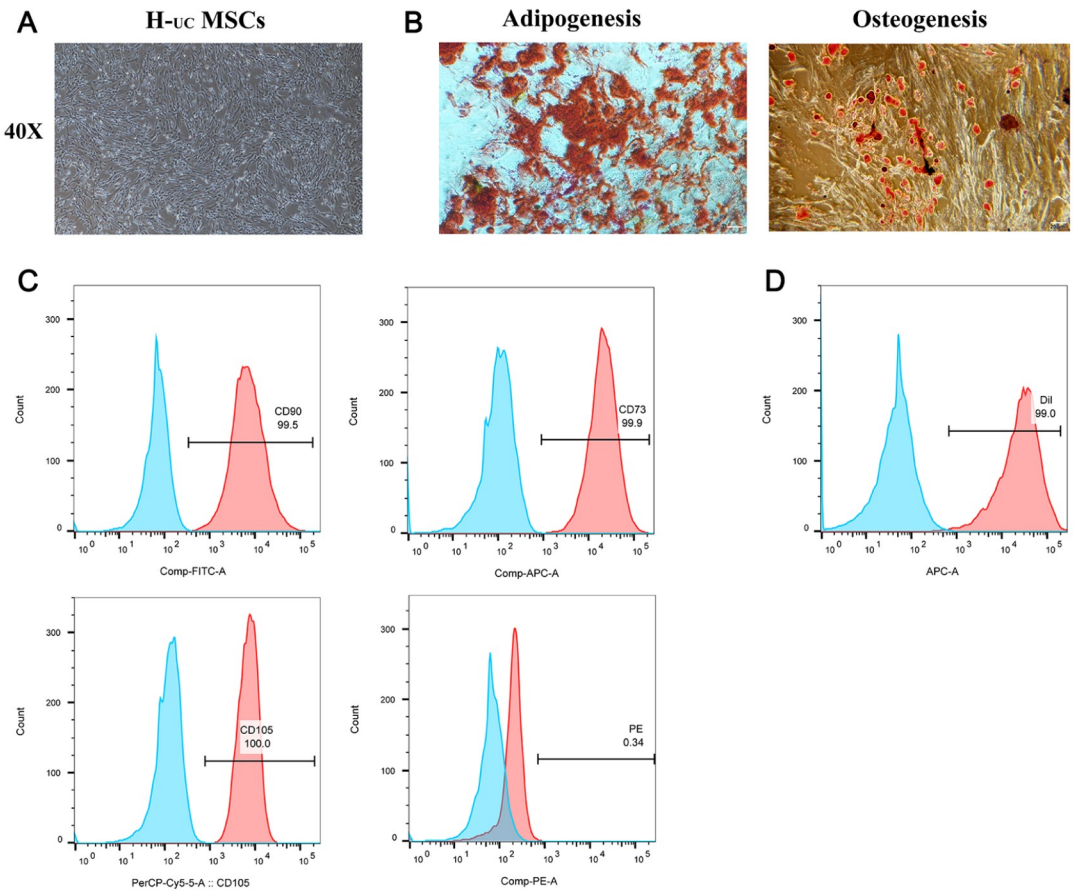

Figure 1. Characterization of H-uc MSCs (A) Optical micrographs of morphological characterization of MSCs at passage 4 (P4). (B) Osteogenic differentiation of MSCs assessed by alizarin red staining. Adipogenic differentiation of MSCs assessed by Oil Red O staining. The magnification is 200×. (C) Flow cytometry analysis for specific phenotype markers of MSCs at P4. (D) Flow cytometry analysis of the labelling efficiency of DiI-labelled MSCs.

histopathological changes in ALF, such as moderate and heavy hepatic steatosis and diffuse hepatic necrosis, were observed in the liver tissues from the CCL_4-treated groups under an optical microscope. The liver function indexes AST and ALT were measured, and it was found that the levels of AST and ALT increased as the concentration of CCL_4 increased (Figure 2B). Survival curves were used to describe the survival status of the CCL_4-treated and NC mice. The results showed that the survival rate of mice decreased with increasing CCL_4 concentration, and there was an approximate 50% survival rate in the mice treated with 2.5 mL/kg CCL_4 (Figure 2C). Therefore, 2.5 mL/kg CCL_4 was selected for subsequent experiments. To investigate the impact of ferroptosis on CCL_4-induced ALF, we examined markers of lipid peroxidation and the antioxidant system. We found that after CCL_4 treatment, serum level of MDA and liver tissue level of Ptgs2 were significantly increased (Figure 2D–F). In contrast, serum level of GSH and liver tissue level of Gpx4 were robustly decreased (Figure 2D–F). Iron deposition in tissues is a distinct marker of ferroptosis. Our findings indicated that treatment with CCL_4 resulted in more noticeable iron deposition in the liver compared with the NC group (Figure 2G). Hepcidin expression in the liver was consistently upregulated in CCL_4-treated mice (Figure 2E,F). Taken together, CCL_4-induced ALF changes the factors associated with ferroptosis and increases hepcidin protein level.

Intravenous MSC treatment protected against ferroptosis in ALF mice

To enhance our understanding of the relationship between ferroptosis and MSCs, we employed H-uc MSCs for intervention in CCL_4-treated mice. Hepatomegaly is the most common clinical symptom in patients with acute liver disease [34,35]. Gross examination showed that under the treatment of MSCs, the liver surface of mice changed from gray-white to a ruddy hue, and the size of the liver went from large to small. This indicated that MSCs effectively reversed the increased liver injury in CCL_4-treated mice (Figure 3A). We also observed that treatment with MSCs could accelerate the amelioration of liver function in ALF mouse models (Figure 3B). As shown in Figure 3C, HE staining revealed limited areas of hepatic steatosis and hepatic necrosis in the MSC intervention group. There were also significant changes in the protein levels of classic biomarkers associated with ferroptosis. We found that serum level of MDA and liver tissue level of Ptgs2 were significantly decreased, while serum levels of GSH and Gpx4 were robustly increased in the MSC intervention group (Figure 3D–F). These findings demonstrated that intravenous MSC treatment rapidly restored liver damage and inhibited ferroptosis progression

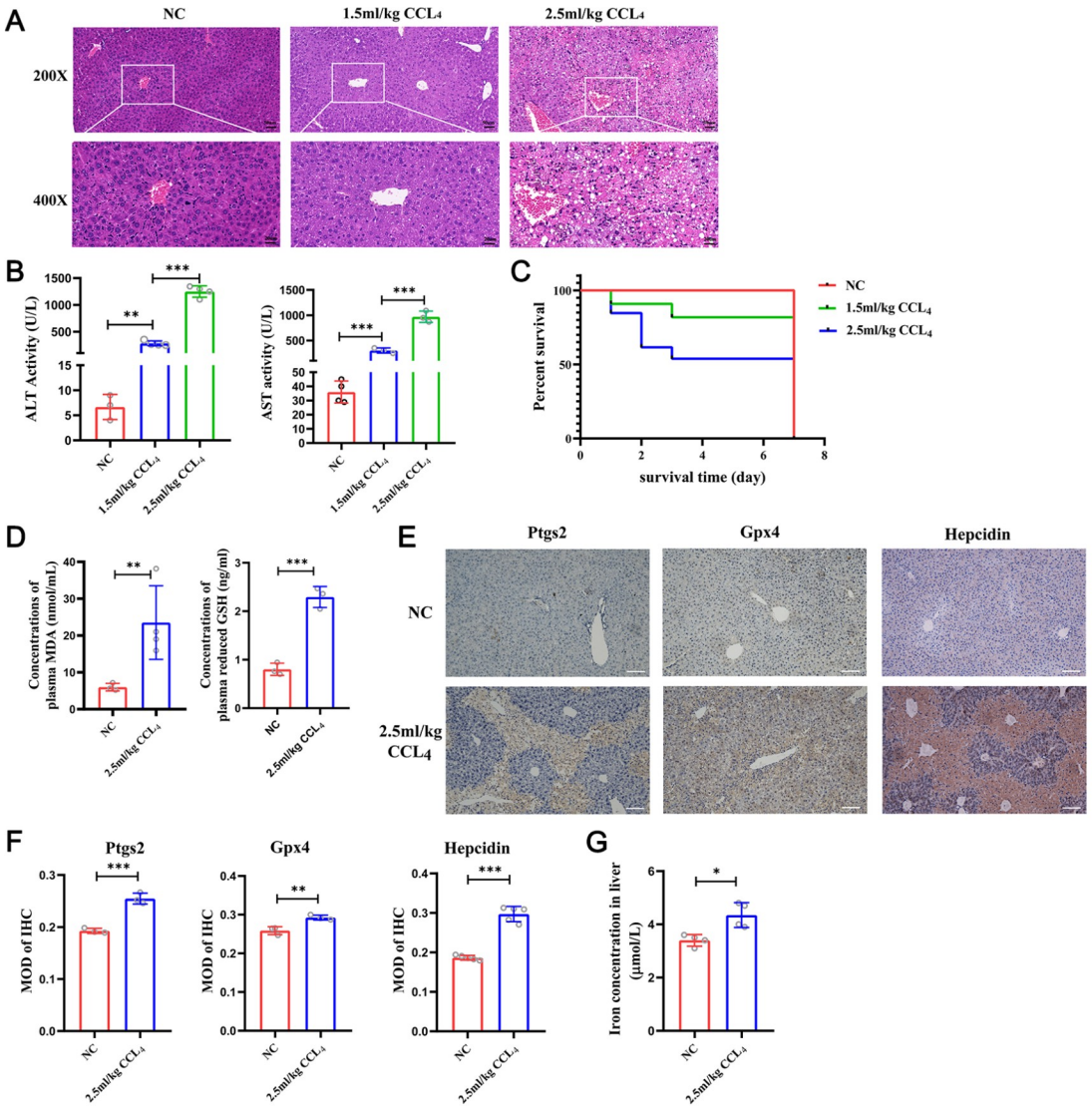

Figure 2. Effects of CCL_4 exposure on liver histoarchitecture and iron homeostasis in mice (A) Representative images of the liver subjected to H&E staining. The magnification is 200× and 400×. (B) The levels of the liver function indexes ALT and AST were measured. (C) Survival curves for mice treated with different concentrations of CCL4. (D) The levels of MDA and GSH in the serum were measured. (E) Immunolocalization of Ptgs2, Gpx4 and hepcidin proteins after CCL_4 exposure. The magnification is 100×. (F) The mean optical density (MOD) of Ptgs2, Gpx4 and hepcidin proteins was calculated from 3 stained pictures of three mice in each group. (G) The level of total iron content in the liver was measured. Data are expressed as the mean ± SEM. ns: no significant difference. $*P<0.05$, $**P<0.01$, and $***P<0.001$.

in CCL_4-induced ALF mice.

MSCs diminished liver iron deposition via the hepcidin-FPN1 axis in ALF mice

Iron homeostasis plays an essential role in the occurrence of ferroptosis. Transporting iron from cells to the extracellular space is an important mechanism for controlling and maintaining iron homeostasis. The iron storage protein ferritin and ferric uptake regulator transferrin receptor 1 (TfR1) were detected by immunohistochemistry. Iron absorption and storage were enhanced in the liver in ALF mice, leading to liver iron deposition (Supplementary Figure S1). As shown in Figure 4A,B, MSC treatment reduced the iron content of liver tissue compared with that in the PBS-treated CCL_4 group. The regulation of hepcidin protein dynamically determines the transport of iron in the body. Immunohistochemical results and western blot analysis indicated that hepcidin protein level was enhanced in the CCL_4 group treated with PBS, but its level was restored after MSC treatment (Figure 4C,D). It should be noted that the increased expression of hepcidin protein directly leads to a decrease in the FPN1 protein level, resulting in a barrier to the output of intracellular iron. Our study also revealed that the correlation between hepcidin and FPN1 expression was increased in response to MSC treatment compared to that in the PBS-treated CCL_4 group, which was contrary to the change in hepcidin level (Figure 4F). These findings indicated that MSCs reduce liver iron content in ALF mice through the hepcidin-FPN1 axis.

Circulating IGF1 is required for the inhibitory effect of MSCs on ferroptosis in ALF mice

Subsequently, we investigated and examined how MSCs exert their

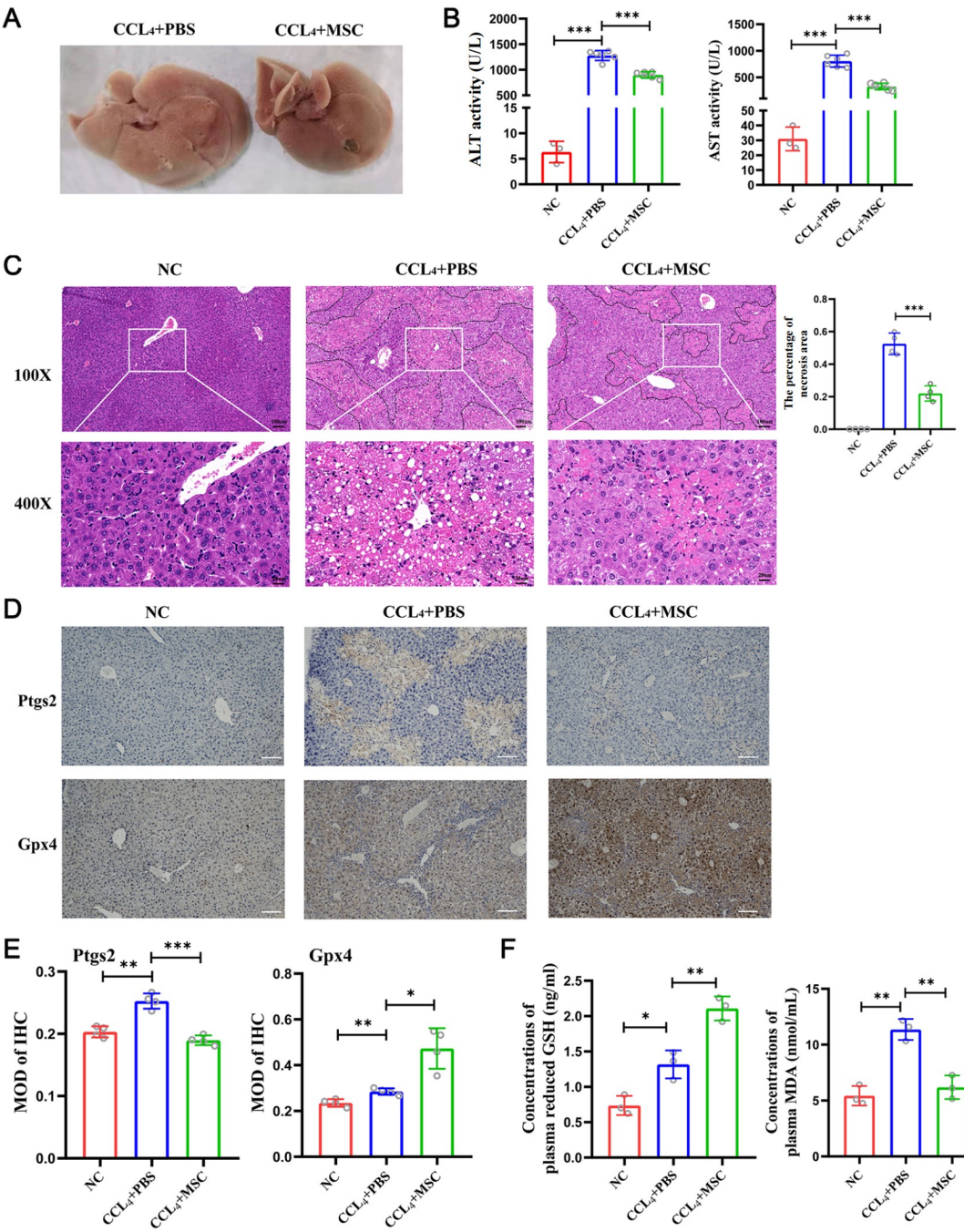

Figure 3. MSC treatment prevented CCL_4-induced ferroptosis in ALF (A) Representative gross morphology images of the liver. (B) The levels of the liver function indexes ALT and AST were measured. (C) Representative images of the liver subjected to H&E staining. The dashed boxes indicate the necrotic area of the liver. The magnification is 100 × and 400 ×. (D,E) Immunolocalization of Ptgs2 and Gpx4 proteins in the NC, CCL_4 + PBS, and CCL_4 + MSC groups ($n = 3$). The magnification is 100 ×. The MOD of Ptgs2 and Gpx4 proteins was calculated from 3 stained pictures of three mice on each group. (F) The levels of MDA and GSH in the serum were measured. Data are expressed as the mean ± SEM. ns: no significant difference. $^*P < 0.05$, $^{**}P < 0.01$, and $^{***}P < 0.001$.

protective potential against CCL_4-induced ferroptosis. To assess the liver distribution of intravenously injected MSCs, immunofluorescence staining of the macrophage marker CD11b was performed. In the liver, Dil-MSCs were distributed in the hepatic sinusoid and showed colocalization with CD11b fluorescence. This result indicated that intravenously injected MSCs could migrate to the liver tissue but were engulfed by macrophages (Figure 5A). Therefore, we hypothesized that MSC treatment exerts a potent therapeutic effect by elevating the release of some factors in the injured body. Considering the significant role of IGF1 in the early stages of repair and regeneration of the liver, we focused on the IGF1 protein. Serum samples were collected from mice in each group, and IGF1 levels were measured by ELISA. Our results showed significantly higher level of serum IGF1 in the MSC

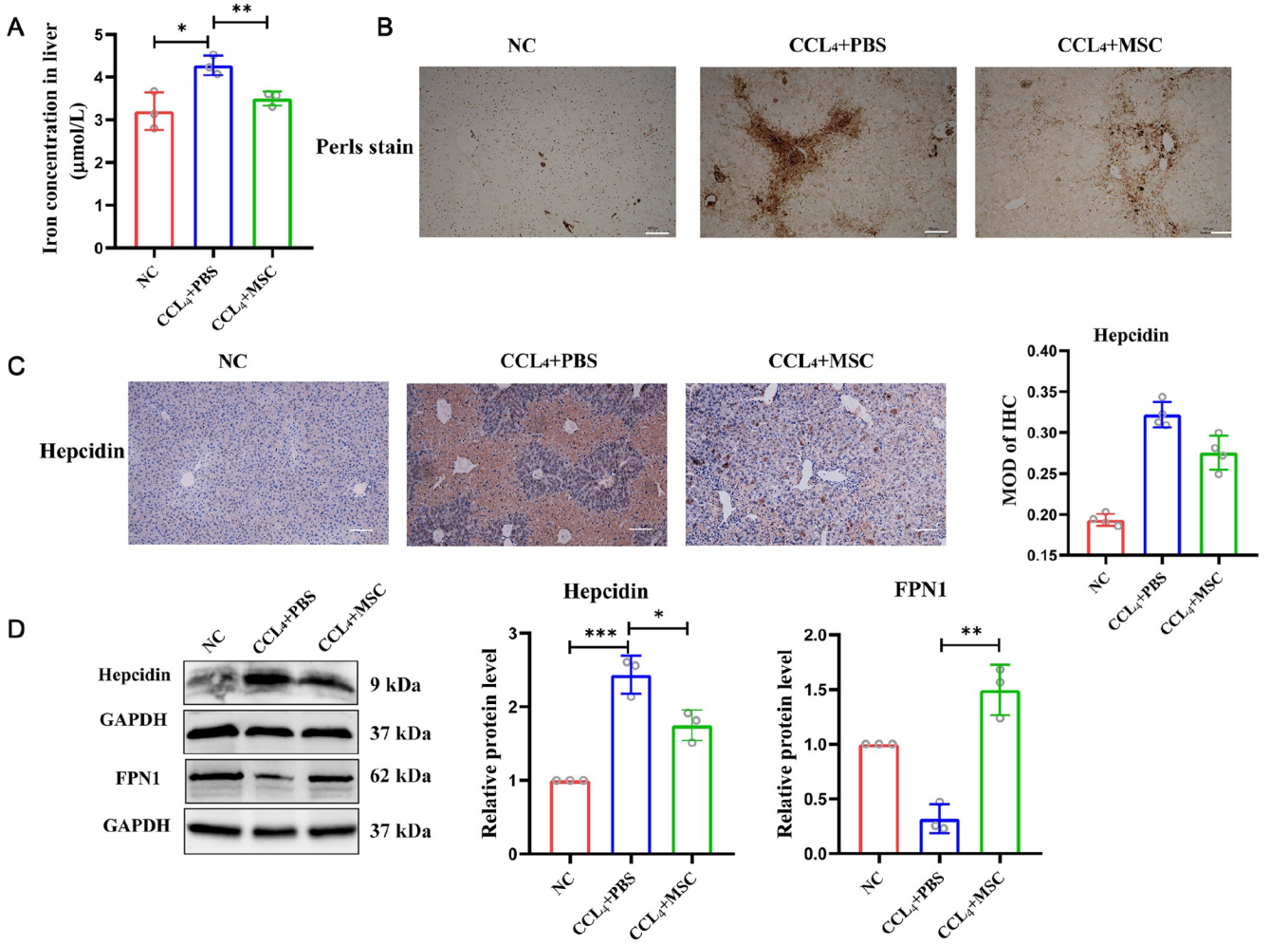

Figure 4. MSC treatment diminished liver iron deposition by regulating the hepcidin-FPN1 axis in ALF mice (A) The level of iron in the liver was measured. (B) Representative images of Prussian blue iron staining in the liver. The magnification is 100×. (C) Immunolocalization of hepcidin protein in the NC, CCL_4 + PBS, and CCL_4 + MSC groups. The magnification is 100×. The MOD of hepcidin protein was calculated from 3 stained pictures of three mice in each group. (D) Western blot analysis of the protein levels of hepcidin, BMP6 and FPN1 in each group ($n = 3$). Data are expressed as the mean ± SEM. ns: no significant difference. *$P < 0.05$, **$P < 0.01$, and ***$P < 0.001$.

treatment model than in the CCL_4-treated groups (Figure 5B). Subsequently, we assessed the expression changes of related molecules in the IGF1-IGF-1R system after MSC treatment. Immunohistochemical staining of the liver revealed increased expression of IGF-1R in the group treated with MSCs compared to the group treated with PBS (Figure 5C). Next, we administered the IGF1 receptor inhibitor PPP to mice treated with MSCs for three consecutive days via intraperitoneal injections and confirmed the role of IGF1 in MSC treatment efficacy by blocking the role of IGF1. The ALF with MSC treatment exhibited significantly higher survival rates than the ALF with MSC and PPP treatments (Figure 5D). Furthermore, we observed further exacerbation of ferroptosis in the PPP groups. As shown in Figure 5E–G, serum level of MDA and liver tissue level of Ptgs2 were downregulated in the CCL_4-MSCs-vehicle group compared with the CCL_4-MSCs-PPP group, while the changes in serum level of GSH and liver tissue level of Gpx4 were significantly reversed upon comparison between the CCL_4-MSCs-PPP group and the CCL_4-MSCs-vehicle group. These findings indicated that IGF1 plays an essential role in MSC treatment against ferroptosis in ALF mice.

MSCs diminished liver iron deposition via the IGF1-hepcidin-FPN1 axis in ALF mice

To investigate the potential of MSCs in reducing liver iron deposition by modulating circulating IGF1 level, we employed PPP again and measured the total iron content and hepcidin expression. Iron deposition in the liver was significantly exacerbated in the CCL_4-MSCs-PPP group when the role of IGF1 was blocked (Figure 6A,B). As shown in Figure 6C,D, immunofluorescence staining and western blot analysis revealed that hepcidin expression was increased in the inhibitor group even after receiving MSC injections. Furthermore, FPN1 expression in the inhibitor group exhibited an inverse correlation with hepcidin protein level (Figure 6C,D). These results showed that MSCs decreased liver iron content by regulating the IGF1-hepcidin-FPN1 axis in ALF mice.

Discussion

Multiple forms of cell death, including necrosis, apoptosis, and

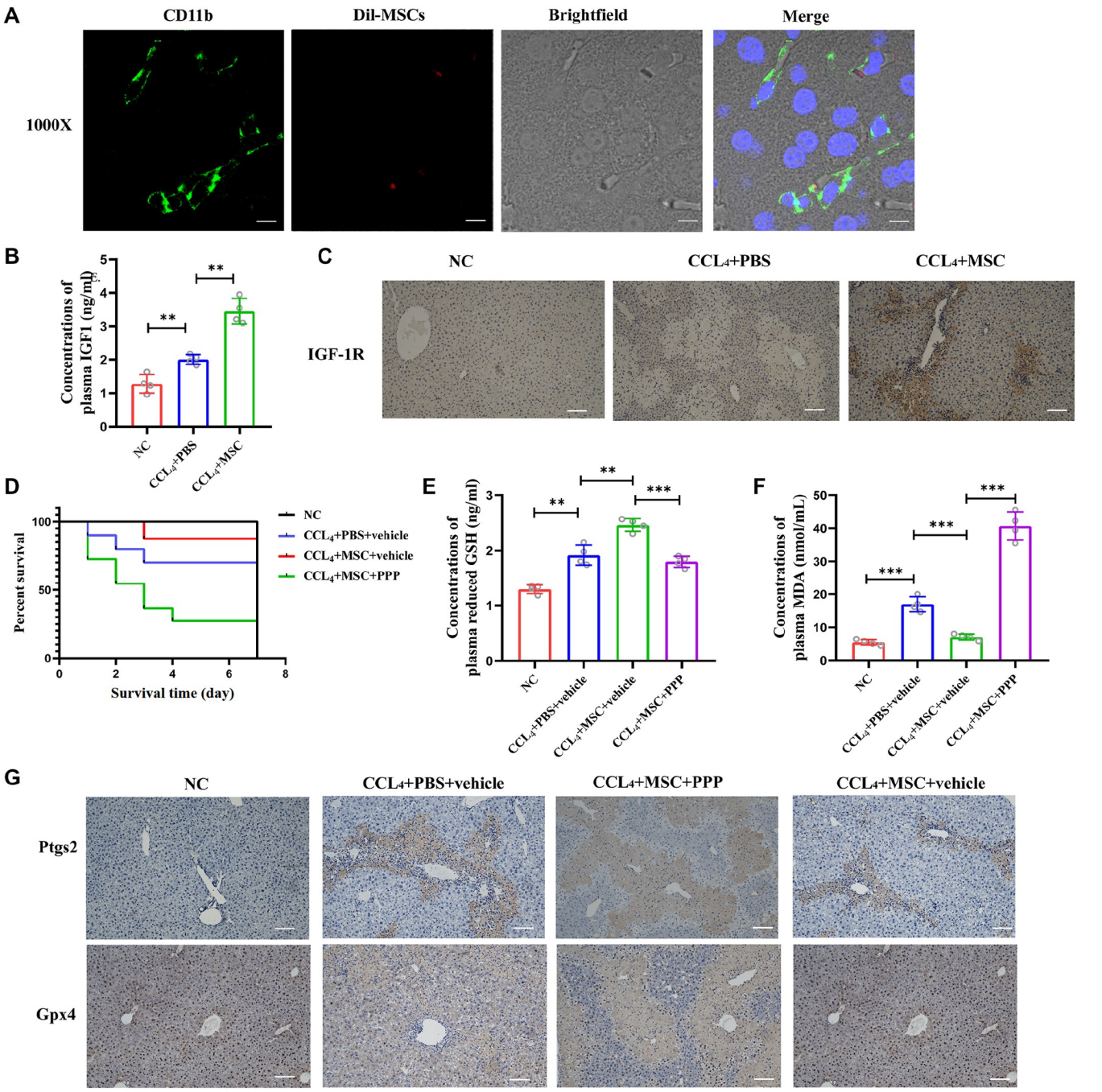

Figure 5. The role of IGF1 in ALF mice with MSC treatment (A) Immunofluorescence staining of the macrophage marker CD11b in the liver. The magnification is 1000 × and 3000 × . (B) Serum IGF1 expression was detected by ELISA. (C) Immunohistochemical staining of IGF-1R proteins in the NC, CCL_4 + PBS, and CCL_4 + MSC groups ($n = 3$). The magnification is 100 × . (D) The survival curves of mice in each group. (E,F) The levels of MDA and GSH were measured. (G) Immunolocalization of Ptgs2 and Gpx4 proteins in the NC, CCL_4 + PBS, and CCL_4 + MSC groups ($n = 3$). The magnification is 100 × . Data are expressed as the mean ± SEM. ns: no significant difference. $^*P < 0.05$, $^{**}P < 0.01$, and $^{***}P < 0.001$.

necroptosis, take part in the occurrence and progression of liver injury. For example, Guo *et al.* [36] demonstrated that the absence of MLKL alleviates liver fibrosis by suppressing hepatocyte necroptosis. Moreover, apoptosis and autophagy also play significant roles in CCL_4-induced hepatocellular injury [37–40]. Since the liver is the main organ of the human body for storing iron, we primarily focused on the mechanistic basis of ferroptosis in ALF. Sun *et al.* [41] demonstrated that targeting ferroptosis was a new challenge and opportunity as a potential strategy for treating ferroptosis-related diseases. Upregulating the expression of GPX4 could diminish ferroptosis in hepatocellular carcinoma [42,43]. Wei *et al.* [44] demonstrated that aqueous extracts of M. mori fructus attenuate CCL_4-induced liver injury by inhibiting ferroptosis via the Nrf2 pathway. In this study, an acute and critical ALF mouse model

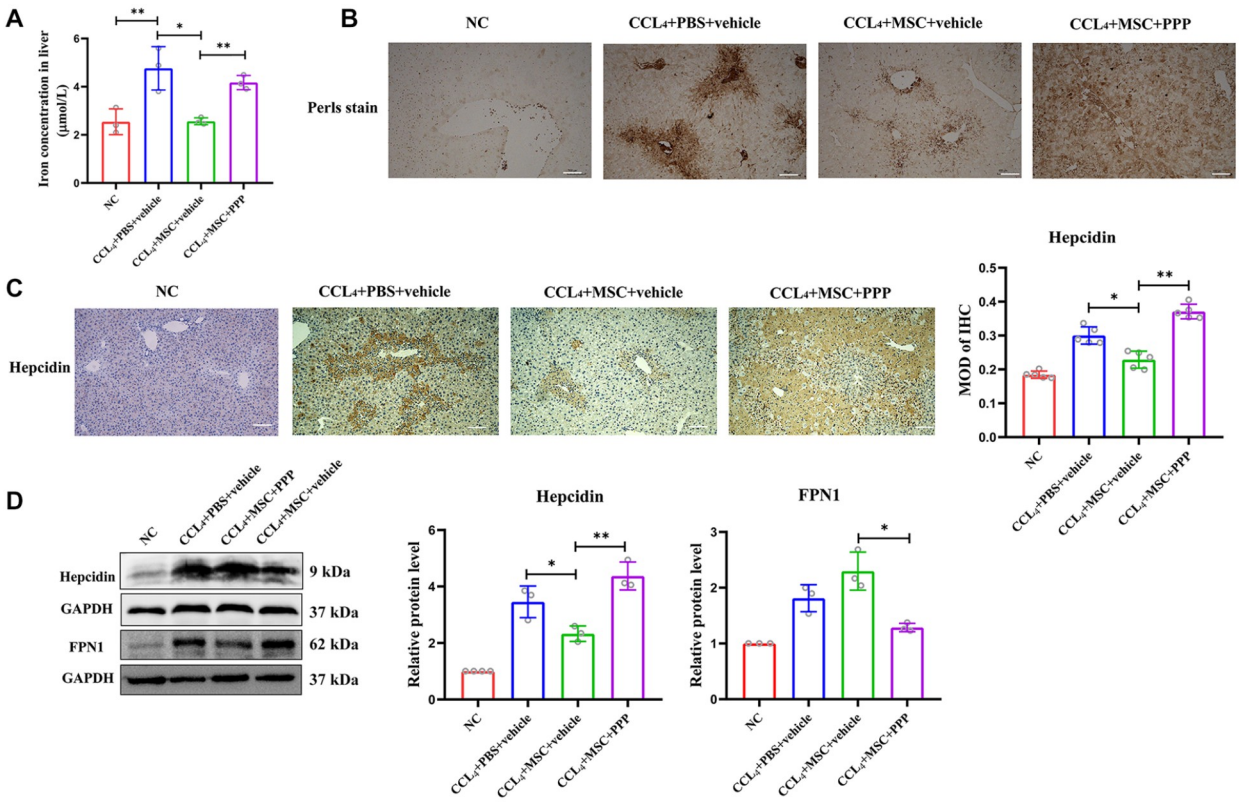

Figure 6. The role of IGF1 in iron deposition in ALF mice treated with MSCs (A) The level of iron in the liver was measured. (B) Representative images of Prussian blue iron staining. The magnification is 100×. (C) Immunolocalization of hepcidin protein in each group. The magnification is 100×. The MOD of hepcidin protein was calculated from 3 stained pictures of three mice in each group. (D) Western blot analysis of hepcidin and FPN1 protein levels in each group ($n=3$). Data are expressed as the mean ± SEM. ns: no significant difference. *$P<0.05$, **$P<0.01$, and ***$P<0.001$.

was established. In addition to the increasing region of hepatic steatosis and hepatic necrosis, ALF livers also experienced significant iron deposition, imbalances in the anti-redox system, and accumulation of lipid peroxides. Furthermore, the therapeutic effect of MSC treatment was observed in reducing lipid peroxide accumulation and iron deposition with increased the antioxidant system level in ALF mice. Our results showed that ferroptosis plays a crucial role in CCL_4-induced ALF, and MSCs have a protective role in resisting ferroptosis.

Excessive iron levels lead to significant cellular dysfunction, especially in liver tissue, which is regarded as the primary organ for iron storage [45]. Ferroptosis has been observed in lipopolysaccharide-induced liver injury, and retinoic acid can protect against liver injury by regulating iron homeostasis [46]. Iron overload exacerbated lipid metabolism disorder and liver injury in rats with nonalcoholic fatty liver disease [47]. Hepcidin is a main regulator of iron homeostasis within hepatocytes and can trigger the degradation of FPN1. FPN1 is the exclusive nonheme iron export protein in mammals [48]. Numerous studies have shown that the dysregulation of hepcidin secretion and altered iron homeostasis impact the progression of liver diseases [49]. Bao *et al.* [50] found that iron overload in hereditary tyrosinemia type 1 induced liver injury through the Sp1/Tfr2/hepcidin axis. Many hepcidin antagonists have been explored and reported to have promising therapeutic potential in regulating iron homeostasis [51,52]. In the present study, we found that iron overload existed in the CCL_4-induced ALF mice. Elevated level of hepcidin and reduced FPN1 expression were associated with iron overload in ALF mice. Furthermore, our results showed that MSC treatment played an important role in reducing iron deposition through the downregulation of hepcidin expression and the upregulation of FPN1 expression in ALF mice. Thus, we concluded that MSCs protect against CCL_4-induced liver ferroptosis through the hepcidin-FPN1 axis.

Numerous studies have reported that IGF1 could promote tissue regeneration and improve the recovery function of tissue by preventing oxidative stress [53,54]. Kokoszko *et al.* [55] found that IGF1 can prevent iron-induced oxidative damage in iron-sensitive tissues. Our study unequivocally confirmed that blocking IGF1 still exacerbated oxidative damage in ALF mice despite the intravenous injection of MSCs. Additionally, numerous studies have shown that IGF1 positively regulates erythropoiesis by increasing erythroid mass, erythropoietin synthesis, and iron bioavailability [56,57]. Insulin/IGF1 signaling could regulate iron homeostasis in *Caenorhabditis elegans*. Kucic *et al.* [58] showed that MSCs genetically engineered to overexpress IGF1 could enhance cell-based gene therapy for renal failure-induced anemia. In our study, we found that inhibiting IGF1 could increase iron loading status in the livers of ALF mice. Therefore, it is suggested that IGF1 could be related to liver iron homeostasis. The hepcidin level reflects the bioavailability of iron in the body [59,60]. An increasing number of cytokines, including growth hormone, sex hormones, growth differentiation factor 15, hepatocyte growth factor, and epidermal growth factor, have been shown to influence hepcidin level. Only a limited number of studies have demonstrated a negative correlation between the

levels of IGF1 and hepcidin in acromegaly patients and healthy people [61]. Our study confirmed that blocking IGF1 could increase hepcidin level. Additionally, IGF1 may function as one of the suppressors of hepcidin. Although it has been proven that IGF1 has no effect on the induction of hepcidin mRNA by BMP6 *in vitro* [62], hepcidin expression is also regulated by the JAK-STAT signaling in addition to BMP-SMAD signaling [63,64]. Therefore, it is necessary to enhance the experimental design to firmly establish this point in subsequent studies.

In conclusion, our study demonstrates an increased hepcidin level in CCl_4-induced ALF mice compared to NC mice, which may initiate liver iron deposition and lead to ferroptosis in CCl_4-induced ALF mice. Furthermore, we reveal that MSCs possess antiferroptotic effects by increasing IGF1 level in ALF. However, the specific mechanism remains to be further explored.

Supplementary Data

Supplementary data is available at *Acta Biochimica et Biphysica Sinica* online.

Acknowledgement

We appreciate the technical and device support from the Base for Shanxi Key Laboratory of Birth Defect and Cell Regeneration, Shanxi Medical University.

Funding

This work was supported by the grant from the Natural Science Foundation of Shanxi Province (No. 202103021223243).

Conflict of Interest

The authors declare that they have no conflict of interest.

References

1. González-Rodríguez Á, Reibert B, Amann T, Constien R, Rondinone CM, Valverde ÁM. *In vivo* siRNA delivery of Keap1 modulates death and survival signaling pathways and attenuates Concanavalin A-induced acute liver injury in mice. *Dis Model Mech* 2014, 7: 1093–1100
2. Saliba F, Samuel D. Acute liver failure: current trends. *J Hepatol* 2013, 59: 6–8
3. Stravitz RT, Lee WM. Acute liver failure. *Lancet* 2019, 394: 869–881
4. Riordan S, Williams R. Perspectives on liver failure: past and future. *Semin Liver Dis* 2008, 28: 137–141
5. Wendon J, Cordoba J, Dhawan A, Larsen FS, Manns M, Nevens F, Samuel D, ***et al.*** EASL Clinical Practical Guidelines on the management of acute (fulminant) liver failure. *J Hepatol* 2017, 66: 1047–1081
6. Dixon SJ, Lemberg KM, Lamprecht MR, Skouta R, Zaitsev EM, Gleason CE, Patel DN, ***et al.*** Ferroptosis: an iron-dependent form of nonapoptotic cell death. *Cell* 2012, 149: 1060–1072
7. Chen J, Li X, Ge C, Min J, Wang F. The multifaceted role of ferroptosis in liver disease. *Cell Death Differ* 2022, 29: 467–480
8. Stockwell BR. Ferroptosis turns 10: emerging mechanisms, physiological functions, and therapeutic applications. *Cell* 2022, 185: 2401–2421
9. Liao Z, Tong B, Ou Z, Wei J, Lei M, Yang C. The role of extracellular vesicles in iron homeostasis and ferroptosis: focus on musculoskeletal diseases. *Traffic* 2023, 24: 384–396
10. Gao M, Monian P, Quadri N, Ramasamy R, Jiang X. Glutaminolysis and transferrin regulate ferroptosis. *Mol Cell* 2015, 59: 298–308
11. Xie Y, Hou W, Song X, Yu Y, Huang J, Sun X, Kang R, ***et al.*** Ferroptosis: process and function. *Cell Death Differ* 2016, 23: 369–379
12. Pigeon C, Ilyin G, Courselaud B, Leroyer P, Turlin B, Brissot P, Loréal O. A new mouse liver-specific gene, encoding a protein homologous to human antimicrobial peptide hepcidin, is overexpressed during iron overload. *J Biol Chem* 2001, 276: 7811–7819
13. Aschemeyer S, Qiao B, Stefanova D, Valore EV, Sek AC, Ruwe TA, Vieth KR, ***et al.*** Structure-function analysis of ferroportin defines the binding site and an alternative mechanism of action of hepcidin. *Blood* 2018, 131: 899–910
14. Li L, Holscher C, Chen BB, Zhang ZF, Liu YZ. Hepcidin treatment modulates the expression of divalent metal transporter-1, ceruloplasmin, and ferroportin-1 in the rat cerebral cortex and hippocampus. *Biol Trace Elem Res* 2011, 143: 1581–1593
15. Zhang H, Ostrowski R, Jiang D, Zhao Q, Liang Y, Che X, Zhao J, ***et al.*** Hepcidin promoted ferroptosis through iron metabolism which is associated with DMT1 signaling activation in early brain injury following subarachnoid hemorrhage. *Oxid Med Cell Longev* 2021, 2021: 9800794
16. Ganz T. Hepcidin, a key regulator of iron metabolism and mediator of anemia of inflammation. *Blood* 2003, 102: 783–788
17. Nicolas G, Bennoun M, Porteu A, Mativet S, Beaumont C, Grandchamp B, Sirito M, ***et al.*** Severe iron deficiency anemia in transgenic mice expressing liver hepcidin. *Proc Natl Acad Sci USA* 2002, 99: 4596–4601
18. De Domenico I, Ward DMV, Nemeth E, Vaughn MB, Musci G, Ganz T, Kaplan J. The molecular basis of ferroportin-linked hemochromatosis. *Proc Natl Acad Sci USA* 2005, 102: 8955–8960
19. Zheng H, Guo X, Kang S, Li Z, Tian T, Li J, Wang F, ***et al.*** Cdh5-mediated Fpn1 deletion exerts neuroprotective effects during the acute phase and inhibitory effects during the recovery phase of ischemic stroke. *Cell Death Dis* 2023, 14: 161
20. Tian H, Xiong Y, Zhang Y, Leng Y, Tao J, Li L, Qiu Z, ***et al.*** Activation of NRF2/FPN1 pathway attenuates myocardial ischemia–reperfusion injury in diabetic rats by regulating iron homeostasis and ferroptosis. *Cell Stress Chaperones* 2021, 27: 149–164
21. Ma JF, Gao JP, Shao ZW. Acute liver failure: a systematic review and network meta-analysis of optimal type of stem cells in animal models. *World J Stem Cells* 2023, 15: 1–14
22. Wang YH, Chen EQ. Mesenchymal stem cell therapy in acute liver failure. *Gut Liver* 2023, 17: 674–683
23. Jin Y, Zhang J, Xu Y, Yi K, Li F, Zhou H, Wang H, ***et al.*** Stem cell-derived hepatocyte therapy using versatile biomimetic nanozyme incorporated nanofiber-reinforced decellularized extracellular matrix hydrogels for the treatment of acute liver failure. *Bioactive Mater* 2023, 28: 112–131
24. Wei H, Li F, Xue T, Wang H, Ju E, Li M, Tao Y. MicroRNA-122-functionalized DNA tetrahedron stimulate hepatic differentiation of human mesenchymal stem cells for acute liver failure therapy. *Bioactive Mater* 2023, 28: 50–60
25. Lin F, Chen W, Zhou J, Zhu J, Yao Q, Feng B, Feng X, ***et al.*** Mesenchymal stem cells protect against ferroptosis via exosome-mediated stabilization of SLC7A11 in acute liver injury. *Cell Death Dis* 2022, 13: 271
26. Zuo H, Wang Y, Yuan M, Zheng W, Tian X, Pi Y, Zhang X, ***et al.*** Small extracellular vesicles from HO-1-modified bone marrow-derived mesenchymal stem cells attenuate ischemia-reperfusion injury after steatotic liver transplantation by suppressing ferroptosis via miR-214-3p. *Cell Signal* 2023, 109: 110793
27. Yu Y, Wu T, Lu Y, Zhao W, Zhang J, Chen Q, Ge G, ***et al.*** Exosomal thioredoxin-1 from hypoxic human umbilical cord mesenchymal stem cells inhibits ferroptosis in doxorubicin-induced cardiotoxicity via mTORC1 signaling. *Free Radical Biol Med* 2022, 193: 108–121
28. Xu J, Wang X, Chen J, Chen S, Li Z, Liu H, Bai Y, ***et al.*** Embryonic stem cell-derived mesenchymal stem cells promote colon epithelial integrity

and regeneration by elevating circulating IGF-1 in colitis mice. *Theranostics* 2020, 10: 12204–12222
29. Wang H, Ba T, Wang Q, Yang L, Li C, Hao X, Yin Y, ***et al.*** Human umbilical cord mesenchymal stem cells attenuate severe burn-induced multiple organ injury via potentiating IGF-1 and BCL-2/BAX Pathway. *Stem Cells Int* 2022, 2022: 5474289
30. Kasprzak A, Adamek A. The insulin-like growth factor (IGF) signaling axis and hepatitis C virus-associated carcinogenesis (Review). *Int J Oncol* 2012, 41: 1919–1931
31. Bonefeld K, Møller S. Insulin-like growth factor-I and the liver. *Liver Int* 2011, 31: 911–919
32. Morales-Garza LA, Puche JE, Aguirre GA, Muñoz Ú, García-Magariño M, De la Garza RG, Castilla-Cortazar I. Experimental approach to IGF-1 therapy in CCl4-induced acute liver damage in healthy controls and mice with partial IGF-1 deficiency. *J Transl Med* 2017, 15: 96
33. Fu YS, Cheng YC, Lin MYA, Cheng H, Chu PM, Chou SC, Shih YH, ***et al.*** Conversion of human umbilical cord mesenchymal stem cells in Wharton's jelly to dopaminergic neurons in vitro: potential therapeutic application for parkinsonism. *Stem Cells* 2006, 24: 115–124
34. Fernandes DA, Assis-Mendoca GR, Costa LBE, Freitas LLL, Boin IFFS, Reis F. Amyloidosis: a rare cause of severe acute liver failure. *Rev Esp Enferm Dig* 2023, 116
35. Kim HJ, Tomaszewski M, Lam EC, Xiong W, Moosavi S. Amyloidosis: a rare cause of severe cholestasis and acute liver failure. *ACG Case Rep J* 2020, 7: e00479
36. Guo R, Jia X, Ding Z, Wang G, Jiang M, Li B, Chen S, ***et al.*** Loss of MLKL ameliorates liver fibrosis by inhibiting hepatocyte necroptosis and hepatic stellate cell activation. *Theranostics* 2022, 12: 5220–5236
37. Zhang Y, Wang Y, Zhang K, Liang X, Guan J, Jin J, Zhang Y, ***et al.*** Profile of 5-HT2A receptor involved in signaling cascades associated to intracellular inflammation and apoptosis in hepatocytes and its role in carbon tetrachloride-induced hepatotoxicity. *Cell Signal* 2023, 105: 110612
38. Tong H, Wang L, Shi J, Jin H, Zhang K, Bao Y, Wu Y, ***et al.*** Upregulated miR-322-5p regulates cell cycle and promotes cell proliferation and apoptosis by directly targeting Wee1 in mice liver injury. *Cell Cycle* 2022, 21: 2635–2650
39. Liu Z, Wu X, Wang Q, Li Z, Liu X, Sheng X, Zhu H, ***et al.*** CD73-adenosine A1R axis regulates the activation and apoptosis of hepatic stellate cells through the PLC-IP3-Ca^{2+}/DAG-PKC signaling pathway. *Front Pharmacol* 2022, 13: 922885
40. Shi B, Wang W, Ye M, Liang M, Yu Z, Zhang Y, Liu Z, ***et al.*** Spermidine suppresses the activation of hepatic stellate cells to cure liver fibrosis through autophagy activator MAP1S. *Liver Int* 2023, 43: 1307–1319
41. Sun S, Shen J, Jiang J, Wang F, Min J. Targeting ferroptosis opens new avenues for the development of novel therapeutics. *Sig Transduct Target Ther* 2023, 8: 372
42. Zhai H, Zhong S, Wu R, Mo Z, Zheng S, Xue J, Meng H, ***et al.*** Suppressing circIDE/miR-19b-3p/RBMS1 axis exhibits promoting-tumour activity through upregulating GPX4 to diminish ferroptosis in hepatocellular carcinoma. *Epigenetics* 2023, 18: 2192438
43. Meng H, Li R, Xie Y, Mo Z, Zhai H, Zhang G, Liang G, ***et al.*** Nanoparticles mediated circROBO1 silencing to inhibit hepatocellular carcinoma progression by modulating miR-130a-5p/CCNT2 axis. *Int J Nanomedicine* 2023, 18: 1677–1693
44. Wei Y, Gao C, Wang H, Zhang Y, Gu J, Zhang X, Gong X, ***et al.*** Mori fructus aqueous extracts attenuates liver injury by inhibiting ferroptosis via the Nrf2 pathway. *J Anim Sci Biotechnol* 2023, 14: 56
45. Tsuchiya H, Akechi Y, Ikeda R, Nishio R, Sakabe T, Terabayashi K, Matsumi Y, ***et al.*** Suppressive effects of retinoids on iron-induced oxidative stress in the liver. *Gastroenterology* 2009, 136: 341–350.e8
46. Lai X, Wu A, Bing Y, Liu Y, Luo J, Yan H, Zheng P, ***et al.*** Retinoic acid protects against lipopolysaccharide-induced ferroptotic liver injury and iron disorders by regulating Nrf2/HO-1 and RARβ signaling. *Free Radical Biol Med* 2023, 205: 202–213
47. Zhang L, Dai X, Wang L, Cai J, Shen J, Shen Y, Li X, ***et al.*** Iron overload accelerated lipid metabolism disorder and liver injury in rats with non-alcoholic fatty liver disease. *Front Nutr* 2022, 9: 961892
48. Nemeth E, Ganz T. Hepcidin-ferroportin interaction controls systemic iron homeostasis. *Int J Mol Sci* 2021, 22: 6493
49. Bloomer SA, Brown KE. Hepcidin and iron metabolism in experimental liver injury. *Am J Pathol* 2021, 191: 1165–1179
50. Bao WD, Fan Y, Deng YZ, Long LY, Wang J, Guan DX, Qian ZY, ***et al.*** Iron overload in hereditary tyrosinemia type 1 induces liver injury through the Sp1/Tfr2/hepcidin axis. *J Hepatol* 2016, 65: 137–145
51. Theurl I, Schroll A, Sonnweber T, Nairz M, Theurl M, Willenbacher W, Eller K, ***et al.*** Pharmacologic inhibition of hepcidin expression reverses anemia of chronic inflammation in rats. *Blood* 2011, 118: 4977–4984
52. Poli M, Girelli D, Campostrini N, Maccarinelli F, Finazzi D, Luscieti S, Nai A, ***et al.*** Heparin: a potent inhibitor of hepcidin expression *in vitro* and *in vivo*. *Blood* 2011, 117: 997–1004
53. Elis S, Wu YJ, Courtland HW, Sun H, Rosen CJ, Adamo ML, Yakar S. Increased serum IGF-1 levels protect the musculoskeletal system but are associated with elevated oxidative stress markers and increased mortality independent of tissue igf1 gene expression. *Aging Cell* 2011, 10: 547–550
54. Puche JE, Muñoz Ú, García-Magariño M, Sádaba MC, Castilla-Cortázar I. Partial IGF-1 deficiency induces brain oxidative damage and edema, which are ameliorated by replacement therapy. *Biofactors* 2016, 42: 60–79
55. Kokoszko A, Dąbrowski J, Lewiński A, Karbownik-Lewińska M. Protective effects of GH and IGF-I against iron-induced lipid peroxidation in vivo. *Exp Toxicologic Pathol* 2008, 60: 453–458
56. Di Tullio F, Schwarz M, Zorgati H, Mzoughi S, Guccione E. The duality of PRDM proteins: epigenetic and structural perspectives. *FEBS J* 2022, 289: 1256–1275
57. Maggio M, De Vita F, Fisichella A, Lauretani F, Ticinesi A, Ceresini G, Cappola A, ***et al.*** The role of the multiple hormonal dysregulation in the onset of "anemia of aging": focus on testosterone, IGF-1, and thyroid hormones. *Int J Endocrinol* 2015, 2015: 1–22
58. Kucic T, Copland IB, Cuerquis J, Coutu DL, Chalifour LE, Gagnon RF, Galipeau J. Mesenchymal stromal cells genetically engineered to over-express IGF-I enhance cell-based gene therapy of renal failure-induced anemia. *Am J Physiol Renal Physiol* 2008, 295: F488–F496
59. Camaschella C, Nai A, Silvestri L. Iron metabolism and iron disorders revisited in the hepcidin era. *Haematologica* 2020, 105: 260–272
60. Ganz T, Nemeth E. Hepcidin and disorders of iron metabolism. *Annu Rev Med* 2011, 62: 347–360
61. Krygier A, Szczepanek-Parulska E, Cieślewicz M, Wrotkowska E, Chanaj-Kaczmarek J, Ruchała M. Iron homeostasis and hepcidin concentration in patients with acromegaly. *Front Endocrinol* 2021, 12: 788247
62. Goodnough JB, Ramos E, Nemeth E, Ganz T. Inhibition of hepcidin transcription by growth factors. *Hepatology* 2012, 56: 291–299
63. Banerjee S, Katiyar P, Kumar L, Kumar V, Saini SS, Krishnan V, Sircar D, ***et al.*** Black pepper prevents anemia of inflammation by inhibiting hepcidin over-expression through BMP6-SMAD1/IL6-STAT3 signaling pathway. *Free Radical Biol Med* 2021, 168: 189–202
64. Zhang F, Zhao P, Qian Z, Zhong M. Central nervous system inflammation induced by lipopolysaccharide up-regulates hepatic hepcidin expression by activating the IL-6/JAK2/STAT3 pathway in mice. *Front Nutr* 2021, 8: 649640